[6]Tsai, S. W., and Wu, E. M., "A General Theory of Strength for Anisotropic Materials," *Journal of Composite Materials*, Vol. 5, Jan. 1971, pp. 58–80.
[7]Tsai, S. W., and Hahn, H. T., *Introduction to Composite Materials*, Technomic, Westport, CT, 1980.
[8]Jones, R. M., *Mechanics of Composite Materials*, Hemisphere, New York, 1975.
[9]Wang, J. T. S., and Dickson, J. N., "Interlaminar Stresses in Symmetric Composite Laminates," *Journal of Composite Materials*, Vol. 12, Oct. 1978, pp. 390–402.

Analysis of Thick Multilayered Anisotropic Plates by a Higher Order Plate Element

Marco Di Sciuva* and Ugo Icardi†
Politecnico di Torino, 10129 Turin, Italy

I. Introduction

In two-dimensional approaches, laminated anisotropic plates and shells have been extensively studied by means of the classical lamination plate theory (CLPT) and the first-order shear deformation theory (FSDT).

The fact that some important modes of failure are related to interlaminar stresses motivated researchers to search for higher order modeling approaches that will serve the purpose of giving predictions of acceptable accuracy and at the same time will be capable of being implemented in practice.

In the literature are found a number of higher order shear deformable models; these models can be grouped into three categories[1] as follows. 1) Approaches based on an assumed global (i.e., for the whole laminate) nonlinear distribution along the thickness of the in-plane displacements or the transverse shearing stresses (smeared laminate models). Since the power expansions in the x_3 coordinate belong to the C^1 class of functions at least (continuity of functions and their first derivative), incompatible transverse stresses appear at interfaces of adjacent layers if the layers have different mechanical properties. 2) Approaches based on an assumed piecewise displacement or stress distribution in the thickness direction (discrete-layer models). Most of the models of this class impose continuity conditions as constraint conditions on each layer, resulting in the number of governing equations increasing with the number of layers in the laminate. 3) Zig-zag models based on piecewise linear or nonlinear through-the-thickness displacement distributions having discontinuous derivatives to allow for appropriate jumps in the strain and stress using the same number of displacement variables as in the corresponding smeared laminate models. In the following we will be interested in the zig-zag models. Specifically, we will make reference to the general formulation recently given by Di Sciuva.[2] The development of shear deformable, multilayered anisotropic plate finite elements follows the same path as in the analytical modeling approaches. For a review of the extensive bibliography on the subject, see the references quoted in Refs. 3–5. In effect, as a basis for the formulation of plate elements of this type, many investigators have employed the smeared laminate models, whereas others make use of the discrete-layer models. In the first approach, the multilayered anisotropic plate element is reduced to an equivalent single anisotropic layer element. Many of the finite element formulations belonging to the second group make use of at least one solid or plate element per layer in the thickness direction. Then this approach requires numerous unknowns, and as a consequence, these formulations become nontractable in the solution of practical engineering problems. The multilayered anisotropic plate finite elements formulated on the basis of the zig-zag plate models overcome this drawback because the number of nodal parameters is independent of the number of layers.[3,5]

Based on the refined third-order zig-zag plate model, Di Sciuva et al.[4] recently formulated an eight-noded general quadrilateral plate element with 56 degrees of freedom (DOF): 10 DOF of the corner nodes (the two in-plane displacements, the two shear rotations, the transverse displacement and its first and second derivatives) and 4 DOF per midside node (the two in-plane displacements and the two shear rotations). Thus, this plate element is characterized by a quadratic variation of the in-plane displacements and shear rotations and quintic variation of the transverse displacement in the element. Only preliminary numerical results were given in Ref. 4. The purpose of the present Note is twofold: 1) to give a brief review of a recent generalization of the zig-zag approach to anisotropic multilayered plates of general lay-ups and 2) to further substantiate the accuracy of the developed eight-noded, curvilinear quadrilateral plate element. To this end, finite element solutions for thickness distribution of transverse shear stresses are compared with analytical results from three-dimensional elasticity and other approximate two-dimensional plate models. The numerical investigations performed in previous works and in the present one reveal the superiority of the zig-zag approaches on the other approximate bidimensional models.

II. Multilayered Plate Model

We consider a plate of constant thickness h made of N parallel thin layers of anisotropic materials perfectly bonded together. The thickness of each layer is assumed to be constant and the material to possess a plane of elastic symmetry parallel to the plate reference surface Ω. Material properties and thickness of each layer may be entirely different. Let x_α be a rectangular Cartesian frame[1] on Ω, x_3 being the normal to Ω. (In this Note, if not otherwise specified, the Einsteinian summation convention over repeated indices will be adopted with Latin indices ranging from 1 to 3 and Greek indices ranging from 1 to 2.) In developing a multilayered plate model that fulfills the contact conditions on the transverse shearing stresses, we assume the following displacement field[2] (in developing the plate model, we assume $\sigma_{33} = 0$):

$$\tilde{u}_\alpha(x_j) = u_\alpha(x_j) + U_\alpha(x_j); \qquad \tilde{u}_3(x_j) = u_3^{(0)}(x_\beta) \tag{1}$$

where

$$u_\alpha(x_j) = \sum_{r=0}^{R} L^{(r)}(x_3) u_\alpha^{(r)}(x_\beta) \tag{2}$$

gives the contribution to the in-plane displacement that is continuous with its derivatives with respect to x_3 (this is the classical expansion used in the smeared laminate models);

$$U_\alpha(x_j) = \sum_{k=1}^{N-1} \phi_\alpha^{(k)}(x_\beta)\left[x_3 - x_3^{(k)}\right] H_k \tag{3}$$

gives the contribution to the in-plane displacement that is continuous with respect to x_3, but with jumps in the first derivative at the interfaces between adjacent layers. Here, $H_k = H[x_3 - x_3^{(k)}]$ is the Heaviside unit function and $\phi_\alpha^{(k)}(x_\beta)$ are functions to be determined by satisfying the contact conditions on the transverse shearing stresses at the interfaces. The details of the derivation are given in Di Sciuva.[2] The functions $L^{(r)}(x_3)$ can be given by any set of linearly independent functions, with at least continuous first derivatives with respect to x_3.

As discussed by Di Sciuva,[2] many multilayered plate models proposed in the literature can be obtained as special cases of the previous one. Here we will focus our attention on symmetric laminated plates in bending. For these plates, let the reference surface

Received Oct. 11, 1994; revision received May 5, 1995; accepted for publication Aug. 10, 1995.

*Associate Professor, Department of Aerospace Engineering, Corso Duca degli Abruzzi, 24.
†Senior Researcher, Department of Aerospace Engineering, Corso Duca degli Abruzzi, 24.

be the midsurface of the plate and let the set of the basis functions $L^{(r)}(x_3)$ be

$$L^{(0)}(x_3) = 1; \qquad L^{(1)}(x_3) = x_3 \tag{4}$$

$$L^{(r)}(x_3) = x_3\left[1 - \frac{4^{r-1}}{2r-1}\left(\frac{x_3}{h}\right)^{2(r-1)}\right] \quad \text{for} \quad r = 2, 3, \ldots \tag{5}$$

This set allows us to satisfy the static condition of zero transverse shearing stresses on the bounding surfaces of the laminate. The third-order zig-zag plate model formulated by Di Sciuva[1] follows in a straightforward manner from the general expressions by setting

$$u_\alpha^{(1)}(x_\beta) = -u_{3,\alpha}^{(0)}; \qquad u_\alpha^{(r)}(x_\beta) = 0 \quad \text{per} \quad r \geq 3 \tag{6}$$

in Eq. (2). The result is[2]

$$\tilde{u}_\alpha(x_j) = -x_3 u_{3,\alpha}^{(0)} + f(x_3)g_\alpha + g_\beta \sum_{k=1}^{N-1} b_{\alpha\beta}^{(k)}\left[x_3 - x_3^{(k)}\right]H_k \tag{7}$$

where, to adhere to the notation used by Di Sciuva,[1] we have posed

$$u_\alpha^{(2)}(x_\beta) = g_\alpha(x_\beta); \qquad f(x_3) = L^{(2)}(x_3)$$

$$b_{\alpha\beta}^{(k)} = A_{\alpha\beta}(k, k+1)\left\{1 - 4\left[\frac{x_3^{(k)}}{h}\right]^2\right\} + A_{\alpha\delta}(k, k+1)\sum_{q=1}^{k-1} a_{\delta\beta}^{(2q)} \tag{8}$$

The quantities $A_{\alpha\beta}(k, k+1)$ and $a_{\delta\beta}^{(rq)}$ are depending only on the transverse shear mechanical properties of the constituent layers. Their expressions are given in Di Sciuva.[2] Notice that Eq. (7) is simply a series expansion in x_3 of $\tilde{u}_\alpha$, with basis functions having discontinuous first derivative with respect to x_3 at the interfaces between layers but continuous in the interior of the layers. Substitution of the displacement field into the linear strain-displacement relations and use of the dynamic version of the principle of virtual displacement yield the equations of motion and boundary conditions. They are given in Di Sciuva.[2] We are delighted to note that by setting $b_{\alpha\beta}^{(k)} = 0$, Eq. (7) reduces to that used in the third-order smeared laminate plate model; further, by setting $f(x_3) = x_3$, the displacement field used in the first-order shear deformation plate theory is obtained.

III. Finite Element Formulation

This section summarizes the displacement finite element formulation of the third-order zig-zag plate model discussed in the previous section, Eq. (7). For further details, see Di Sciuva et al.[4]

The plate element formulated on the basis of the third-order zig-zag plate model has 10 DOF at each corner node, and 4 DOF at each midside node, thus giving a total of 56 DOF. For the corner nodes, the nodal parameters are the five generalized displacements[3] u_α, w, g_α, the two total rotations $\partial_\alpha w$, the two curvatures $\partial_{\alpha\alpha} w$, and the twist $\partial_{\alpha\beta} w$ of the reference surface Ω. (To prevent the notation from being cumbersome, we make the following change in notation: $u_\alpha^{(0)} \equiv u_\alpha$ and $u_3^{(0)} \equiv w$.) For the midside nodes, the nodal parameters are the two in-plane displacements u_α and the two shear rotations g_α. In the sequel, this plate element will be named RHQ56.

Notice that the finite element formulation based on the displacement approach for the plate model here considered requires C^1 approximation of the transverse deflection w, and C^0 approximation of the in-plane displacements u_α and of the shear rotations g_α. Thus, we have used the tensor product of Hermite quintic polynomials as interpolation functions for w, and the following serendipity interpolation functions for u_α and g_α:

$$\mathcal{N}_i = \tfrac{1}{4}(1 + \xi_i\xi)(1 + \eta_i\eta)(\xi_i\xi + \eta_i\eta - 1) \quad \text{for} \quad i = 1, 2, 3, 4$$

$$\mathcal{N}_i = \left(\eta_i^2/2\right)(1 - \xi^2)(1 + \eta_i\eta) + \left(\xi_i^2/2\right)(1 + \xi_i\xi)(1 - \eta^2) \quad \text{for} \quad i = 5, 6, 7, 8$$

where ξ_i and η_i are the coordinates of the nodal point i in the natural plane.

Thus, the RHQ56 plate element is a typical quadratic element (also called serendipity element) for the in-plane displacements and shear rotations. [Notice that following the scheme given at the end of the previous section, it is possible to derive from the RHQ56 plate element the corresponding plate elements formulated on the CLPT, on the FSDT, and on the third-order or higher order shear deformation theory (HSDT).]

Note that the element is able to model a constant strain state and a rigid-body displacement field in the membrane and transverse behavior. (In this last case, a constant strain state is a state at constant curvature or torsion of the midsurface.) In addition, the element is conforming due to the continuity of the displacements and the slopes across adjacent elements.

The formulation is isoparametric for u_α and g_α and subparametric for w.

The formulation of the element elastic stiffness matrix, the consistent mass matrix, and the nodal loads vector follows the quite standard rules of the finite element method and is not given here. Explicit expressions for these matrices are given in Ref. 4.

IV. Numerical Results and Concluding Remarks

To show the accuracy and reliability of the RHQ56 plate element, in the following analytical and finite element results are given for the bending under sinusoidal transverse loading $\bar{p}_3(x_1, x_2) = \bar{p}_0 \sin \pi x_1/a \sin \pi x_2/a$ of a five-layered, symmetric cross-ply (0/90/0/90/0) square plate under special simple support boundary conditions, i.e., supports that allow normal displacements on the boundary but prevent lateral contraction (in other words, hinged edges, free in the in-plane normal direction). The layers have equal thickness and the mechanical properties of the unidirectional layer are $E_L/E_T = 25$, $G_{LT}/E_T = 0.5$, $G_{TT}/E_T = 0.2$, and $\nu_{LT} = 0.25$ (L and T are the directions parallel and normal to the fibers). The plate thickness to span ratio is $a/h = 4$.

Because of the interest in the estimates of the transverse shear stresses, only the thickness-wise distributions of these stresses are plotted. In addition, only the stress distributions predicted by the constitutive lamina relations are quoted. Figure 1 compares the thickness-wise distributions of the transverse shear stress σ_{13} as predicted by the present third-order zig-zag plate model (refined

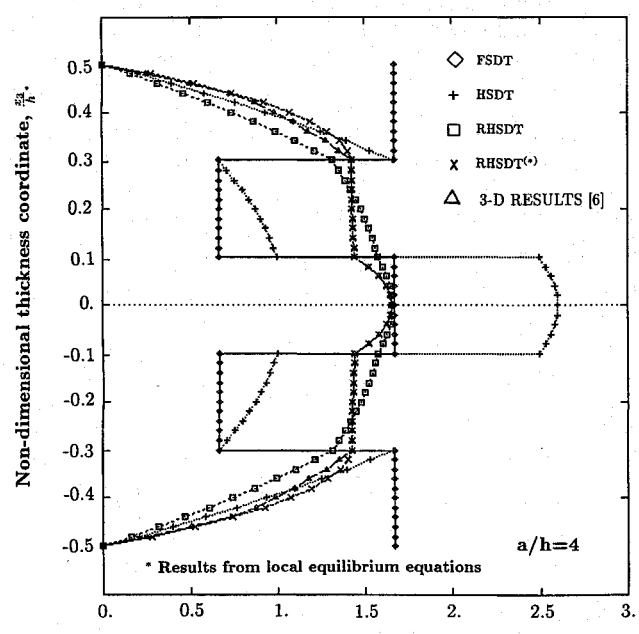

Fig. 1 Thickness-wise distribution of the nondimensional transverse shear stress in a five-layered symmetric cross-ply (0/90/0/90/0) strip under sinusoidal loading, as obtained from constitutive equations: analytical results.

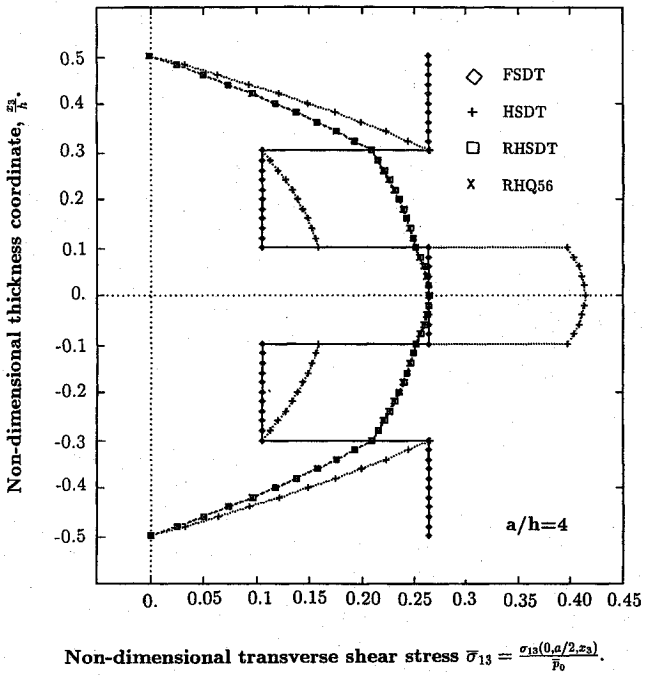

Fig. 2 Thickness-wise distribution of the nondimensional transverse shear stress in a five-layered symmetric cross-ply (0/90/0/90/0) square plate under bisinusoidal loading, as obtained from constitutive equations. Analytical and finite element method results.

HSDT [RHSDT]) with those predicted by the exact elasticity solution[6] and other commonly used bidimensional plate models: FSDT and HSDT. The quoted results refer to the cylindrical bending problem in the (x_1, x_3) plane. This sample problem has been investigated for purpose of comparison with exact elasticity solutions.[6] It is remarkable the very good correlation existing between the estimates of the RHSDT plate model and the exact elasticity solution. On the contrary, notice the inadequacy of all smeared plate models to give acceptable prediction for this quantity. Figure 2 refers to the bending of a square plate and compares analytical and finite element results. Because of symmetry, only one quarter of the plate has been modeled with 5×5 plate elements. All of the results were obtained by using the Gauss quadrature formula with 5×5 integrating points. Notice the high accuracy of the developed plate element. It should be remarked that numerical tests not reproduced here for sake of brevity show that 1) when compared with third-order plate modeling (HSDT), which will not fulfill the continuity stress conditions at the interfaces, the proposed third-order zig-zag approach also improves the prediction of the through-thickness distributions of the in-plane response (in-plane displacements and stresses) and 2) this plate element is practically locking free and behaves well also in distorted configurations.

It is concluded that the proposed approach gives very accurate results for low plate thickness ratios and high relative values of the elastic moduli and does not require any arbitrary shear correction factor. It is of importance to remember that the thickness-wise distributions were obtained from the lamina constitutive equations. It is the authors' opinion that the most important numerical advantage of the third-order zig-zag approach is in the finite element formulation, because continuous thickness-wise distributions of the transverse shear stresses can be obtained without resorting to the integration of the local equilibrium equations. In effect, the last approach requires second derivatives of the displacement field, thus lowering the accuracy of the approximation.

References

[1]Di Sciuva, M., "Multilayered Anisotropic Plate Models with Continuous Interlaminar Stresses," *Composite Structures*, Vol. 22, No. 3, 1992, pp. 149–168.

[2]Di Sciuva, M., "A Generalization of the Zig-Zag Plate Models to Account for General Lamination Configurations," *Atti Accademia delle Scienze di Torino-Classe di Scienze Fisiche, Matematiche e Naturali*, Vol. 28, Fasc. 3–4, 1994, pp. 81–103.

[3]Di Sciuva, M., "A General Quadrilateral Multilayered Anisotropic Plate Element with Continuous Interlaminar Stresses," *Computers and Structures*, Vol. 47, No. 1, 1993, pp. 91–105.

[4]Di Sciuva, M., Icardi, U., and Dobrynin, V., "An Eight Noded Multilayered Plate Element Based on a Refined Discrete-Layer Plate Theory," *Proceedings of the XII Congresso Nazionale AIDAA* (Como, Italy), Italian Association of Aeronautics and Astronautics, Milan, Italy, 1993, pp. 1023–1034.

[5]Di Sciuva, M., "A Third-Order Triangular Multilayered Plate Finite Element with Continuous Interlaminar Stresses," *International Journal for Numerical Methods in Engineering*, Vol. 38, No. 1, 1995, pp. 1–26.

[6]Pagano, N. J., "Exact Solutions for Rectangular Bidirectional Composites and Sandwich Plates," *Journal of Composite Materials*, Vol. 4, Jan. 1970, pp. 20–34.

Ribbed Cylindrical Shells Under a Concentrated Transverse Load

Sıddık Şener*
Gazi University, Ankara 06571, Turkey

Introduction

In this Note, a circular cylindrical shell is assumed to be simply supported. The material behavior of the shell and the rib is linearly elastic, and the material is homogeneous and isotropic. The solution of a ribbed shell under a concentrated load is obtained by considering the shell and the rib separately. The interaction forces, which arise along the contact line between the rib and the shell are expanded in Fourier series, and then the solutions of the ring and the shell under the interaction forces are obtained. The unit displacement matrix is used with the boundary conditions, which gives the unknown amplitudes of the interaction forces. Thus, knowing these amplitudes, the displacements under the loads are obtained from the ring or from the isotropic shell. In this way the analytic solution of the ribbed shell is accomplished. At the end of this Note, a numerical example is discussed and the solution is summarized in the figures and table.

Formulation of the Ribbed Shell

The ends of the shell (Fig. 1) are assumed to be supported with diaphrams (not shown in the figure) that are very rigid in their plane and flexible out of the plane, so that the shell can be considered to be simply supported.

After all parameters of the problem are expressed in Fourier series, the equilibrium equations of the shell are

$$[\Phi]_m\{X\}_m = \{X_0\}_m \tag{1}$$

The unit displacement matrix $[\Phi]$ of the total system includes the rib $[\theta]$ and the isotropic shell $[\Phi_1]$ unit displacement matrices,

$$([\Phi_1] + [\theta])_m\{X\}_m = \{X_0\}_m \tag{2}$$

This expression can be written in the form

$$\left[\begin{bmatrix} w_r & w_t \\ v_r & v_t \end{bmatrix}_{sh} + \begin{bmatrix} w_r & w_t \\ v_r & v_t \end{bmatrix}_{rg}\right]_m \begin{Bmatrix} X_1 \\ X_2 \end{Bmatrix}_m = \begin{Bmatrix} w_0 \\ v_0 \end{Bmatrix}_{sh,m} \tag{3}$$

The unknown quantities X_1 and X_2 denote the amplitudes of the interaction forces and are obtained from Eq. (3). The displacements

Received June 2, 1993; revision received Feb. 4, 1995; accepted for publication Feb. 20, 1995.

*Professor, Department of Civil Engineering.